Earth and Planetary Science Letters, 29 (1976) 309–325

PLUMES, SUBAXIAL PIPE FLOW, AND TOPOGRAPHY ALONG THE MID-OCEANIC RIDGE

PETER R. VOGT

Ocean Floor Analysis Division, U.S. Naval Oceanographic Office, Washington, D.C. (USA)

Received January 6, 1975
Revised version received September 15, 1975

If plate thickness depends on crustal age, the region of extensive partial melting below the spreading axis will be wider around fast-spreading ridges. The melt region creates a subaxial conduit channeling partial melts away from ridge-centered hot spots. The channel is here modeled by an elliptical pipe of semiminor (vertical) axis 2×10^6 cm (20 km) and semimajor (horizontal) axis KS, where S is spreading half-rate (cgs) and K is a constant of magnitude 10^{14} to 10^{15} seconds. This simple analytical model is used to explain the observation that maximum hot spot elevations on the Mid-Oceanic Ridge fall dramatically with increasing spreading rate (there are no Icelands or Afars on the East Pacific Rise!). A hot spot under a fast-spreading ridge has a broad pipe in which to discharge its partial melts; hence, only a slight topographic gradient and a low elevation is needed to discharge the mass flux rising out of the deeper mantle at the hot spot center. A second factor is that partial melts are "used up" faster in the accretion process on fast-spreading ridges. In the simple analytical model, both factors operating together explain the rapid fall of hot spot heights with increasing spreading half-rate. This result indirectly helps confirm the idea of horizontal pipe flow below the Mid-Oceanic Ridge.

A theoretical topographic profile through a hot spot on the Mid-Oceanic Ridge is derived from the assumption that the pressure – i.e., topographic – gradient at a distance x from the hot spot is sufficient to supply all the accreting lithosphere downstream of x, out to x_n, the limit of topographic hot spot influence. The predicted profile is quadratic in x and concave upward, and resembles several observed profiles where neighboring hot spots are not so close as to confuse the profiles. Some observed profiles are more nearly linear or even convex upward. This could be explained, for example, by downstream increases in viscosity or decreases in pipe dimensions.

A hot spot on a ridge spreading at much less than 1 cm/yr half-rate would produce an enormous elevation of the ridge axis, according to our model, because the pipe would be very narrow. Such a large topographic high would create a large gravity potential which would cause the plates to move apart faster, thereby widening the pipe, and reducing the topographic high. The system of ridges and hot spots may thus be self-regulating with respect to plate speeds; this could explain why spreading half-rates on the Mid-Oceanic Ridge are in many areas as low as 1.0 cm/yr but very rarely as low as 0.5 cm/yr.

1. Introduction

A recent comparison of gravity, bathymetry and spreading rate along the Mid-Oceanic Ridge [1] revealed (a) a rather poor but significant positive correlation between free air gravity and differences in crestal depth; (b) no correlation between spreading half-rate and gravity; and (c) no uniform relationship same sign and gradient as predicted for convection in a Newtonian fluid. This observation plus the inability of the lithosphere to support the loads implied by the long-wavelength gravity anomalies lends additional credence to mantle convection below the plates [1].

In this paper we argue that the data compiled by Anderson et al. [1] also support a particular kind of

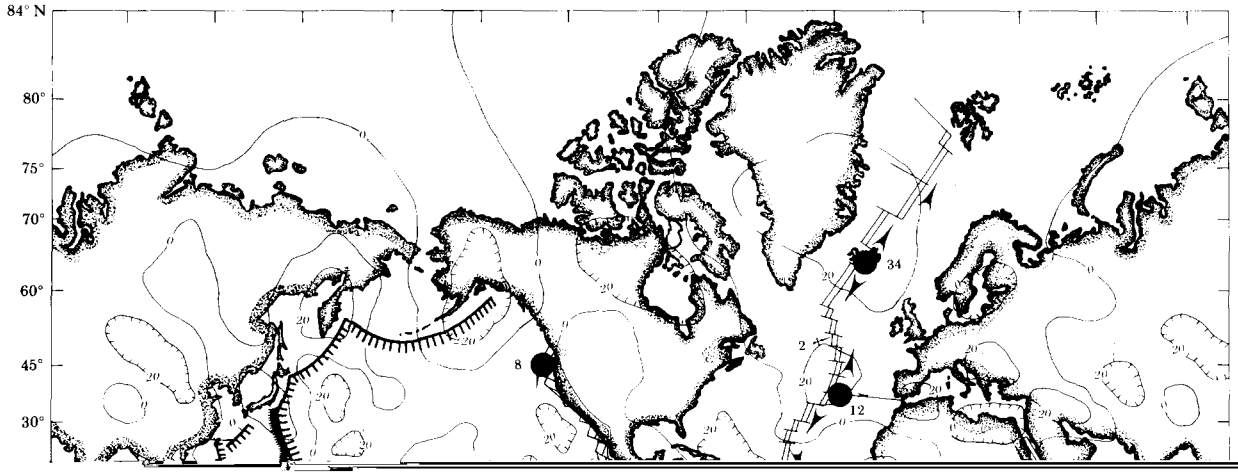
84° N
80°
75°
70°
60°
45°
30°
0
20
8
2
12
34

in places like Iceland, the Azores, the Afar Triangle,

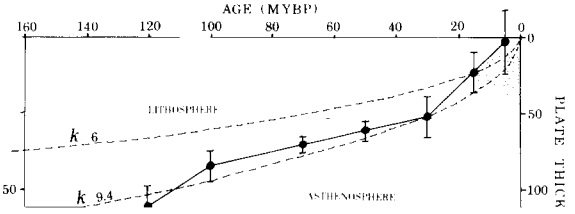

dicted by the plate thickening model. In the interests of developing a simple analytical model we approximate the pipe by an ellipse of vertical, semiminor axis, a = constant and horizontal, semimajor axis, $b = KS$, where K is a constant. From the results of Solomon [19] on the Mid-Atlantic Ridge at 53°N (S = 1 cm/yr) we estimate a = 20 km and $b = KS$ = 40 km. The low-O.

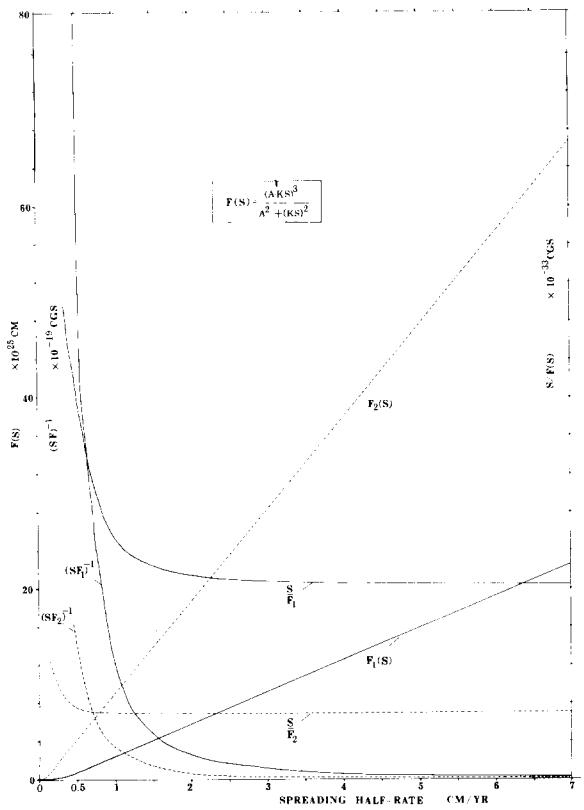

Fig. 4. Spreading rate (S) dependence of several functions used in computing hot spot topographic models using concept of flow in an elliptical pipe of semiminor axis (vertical) a, and semimajor axis (horizontal) KS, where K is either 1.25×10^{14} sec (solid curves) or 3.7×10^{14} sec (dashed curves). K values were estimated from data of Solomon [19], Leeds et al. [20], and Solomon and Julian [21]. Note that as S drops below about 1 cm/yr, both (SF) and S/F rapidly become large. K is not to be confused with constant k describing plate thickening as a function of time (Fig. 3).

one feature to another but no clear dependence on S. We assume for now that there is no S dependence. (In a later section we develop a somewhat different model in which it is explicitly assumed that hot spot discharge is not a function of S and is all used for plate accretion; if this is so x_n is proportional to $1/S$, the lack of a clear observed S dependence being the result of neighboring hot spots not giving actual values of x_n.) If $x_n \neq x_n(S)$ and for topographic bulges of roughly triangular profile [1], we can set:

$$\tan\theta = h_0/x_n$$

Numerical values of $\mu = 0.5 \times 10^{19}$ poises (P), $\rho_m - \rho_w \equiv \Delta\rho = 2.3$ g/cm^3, and $x_n = 2000$ km will be introduced in calculating the pipe flow, which we now write as:

$$Q = \frac{\pi g \Delta\rho h_0}{2x_n\mu} F(S)$$

Now consider a plume of discharge Q developing under a portion of the Mid-Oceanic Ridge. The first effect of this mass supply will be to provide enough material above the plume to accrete new oceanic plate; without the presence of the plume this material would have to be sucked up from deep in the asthenosphere by whatever forces pull the plates apart. Imagine enclosing the plume region by a vertical box whose sides are oriented parallel and perpendicular to the local Mid-Oceanic Ridge. Into the box from below flows a discharge Q, part of which is injected into the bidirectional pipe, as given above, and the balance is used locally to make new lithosphere. This "local accretion flux," moving out of the box at right angles to the pipe flux, is given by $2STL$, where S is spreading rate, T is local plate thickness (~50 km) and L is length of ridge created above the plume (~100 km). For a certain period of time after Q begins, flow out of the box will be less than Q and material will accumulate in the box. This is because initially the topographic bulge is not great enough and the slope not steep enough to move enough material down the "sewer pipe". However, an equilibrium topographic profile must eventually be attained, and we shall henceforth assume that most plumes are in this equilibrium state, for which:

$$Q = 2STL + \frac{\pi g \Delta\rho}{2x_n\mu} h_0 F(S) \qquad (2)$$

Eq. 2 could be solved for $h_0(S)$ if Q were known. To obtain Q, assume that it is constant or varies randomly from one hot spot to another. Let us then ask what Q will give an h_0 of about +2.6 km for $S = 1$ cm/yr (Fig. 2), as observed; we shall than use this same discharge as a constant to calculate $h_0(S)$. At 1 cm/yr, $2STL$ is 0.64×10^7 cm^3/sec (0.2 km^3/yr) and Q is 3.06×10^7 cm^3/sec (0.96 km^3/yr), using the values given previously for the various constants, and $F_1(S)$ from Fig. 4. By rearranging eq. 2:

$$h_0(S) = \frac{(Q - 2STL)}{F(S)} \frac{2\mu x_n}{\pi g \Delta\rho} \qquad (3)$$

and a graph of this function is labelled A in Fig. 2. An adequate fit to the observed $h_0(S)$ is obtained, the main feature being a rapid, nonlinear drop as S increases from 1 to several cm/yr. Physically, this results from an initially rapid increase of flow rate through an elliptical pipe, as horizontal axis, KS, is increased.

In this model we did not assume that the pipe flux feeds the accreting lithosphere over the entire topographic bump out to x_n, or what the flow does after it exits our imaginary box. We used only the empirical observation that bathymetric profiles down rise crests over hot spots are crudely triangular, with wavelength independent of S. In the following section we consider a more restrictive model in which it is assumed that all pipe flux ends up feeding all lithosphere accretion out to x_n from the plume center.

3. The longitudinal topographic profile through a hot spot: the plate feed hypothesis

In the preceding section we have tried to relate the differences in "summit heights" (h_0) of ridge-centered (Icelandic) hot spots to differences in spreading rate, because such differences must control the cross-dimension of the pipe that carries excess partial melts away from the plume. We shall return to this subject later, using somewhat different assumptions. Consider now the longitudinal profile (along the spreading axis) of such a ridge-centered hot spot. Let x be distance from the hot spot center, and $Q(x)$ be volumetric discharge rate through the longitudinal pipe in both directions. At any distance x we can require that sufficient pressure gradient exists to supply enough melts to produce all the lithosphere of thickness T manufactured downstream from x, out to a distance x_n, the limit of hot spot influence. We shall refer to this as the "plate feed hypothesis". If it is assumed that no material from the normal asthenosphere is contributed locally, the by-

and changing the sign of dh/dx to make h decrease with increase in x, we get:

$$Q(x) = -\frac{\pi g \Delta\rho}{4\mu(x)} \frac{dh(x)}{dx} \frac{a^3K^3S^3}{a^2 + K^2S^2} \equiv \frac{-\pi g}{4} \frac{\Delta\rho}{\mu(x)} \frac{dh}{dx} F(S)$$

Therefore:

$$\frac{-\pi g}{4} \frac{\Delta\rho}{\mu(x)} \frac{dh}{dx} F(S) = 2(x_n - x)ST$$

Viscosity is here expressed as a function of x because melt percentage, temperature, and hence viscosity are likely to decrease with increasing x.

Rearranging, we get:

$$\frac{dh}{dx} - \frac{8ST\mu}{\pi g F(S)\Delta\rho} + \frac{8x_nST\mu}{\pi g F(S)\Delta\rho} = 0 \qquad (4)$$

For μ = constant this has the quadratic solution:

$$h(x) = \frac{1}{2} \frac{8\,ST\mu}{\pi g\Delta\rho F(S)} x^2 - \frac{8x_nST\mu}{\pi g\Delta\rho F(S)} x + h_0$$

or:

$$h(x) = \frac{Cx^2S}{2F(S)} - \frac{Cx_nSx}{F(S)} + h_0 \qquad (5)$$

where $C \equiv 8T\mu/\pi g\Delta\rho$ and h_0 is elevation of the center of the hot spot above the reference level.

The slope predicted by this model:

$$\frac{dh}{dx} = \frac{8ST\mu}{\Delta\rho\pi g F(S)} (x - x_n)$$

is steepest at $x = 0$, where it equals $-8ST\mu x_n/\pi g F(S)\Delta\rho$ and the average slope is half this value. (We leave until later the comparison of observed slopes to those calculated by the above formula.) Actually the observed slope is zero in the immediate area of upwelling, and of course eq. 5 is only meant to apply of the order 100 km and more from the center. At $x = x_n$ the slope is zero; the model profile there merges smoothly with the ex-

We now consider whether eq. 5 adequately describes "real" bathymetric profiles along the spreading axis, as a function of distance from a hot spot. Although eq. 4 requires that $dh/dx = 0$ at $x = x_n$, it says nothing about $h(x_n)$. If the constants are correct, $h(x_n)$ should equal zero, and this requirement imposes a constraint on the constants, for $h(x_n) = 0$ only if $h_0 = \frac{1}{2} CS/F \cdot x_n^2$, where $C = 8T\mu/\pi g\Delta\rho$. If this condition is met, all the profiles will have the form:

$$h(x) = h_0 \frac{x^2}{x_n^2} - 2h_0 \frac{x}{x_n} + h_0$$

We defer the question of meeting this requirement until later and assume for now that reasonable values of constants can be found and that the curves can be constrained by observed values of h_0 and x_n for each hot spot. The observed bathymetric profiles $h(x)$ should exhibit "quadratic" curvature (concave upward) if they conform to the model. Fig. 5 shows that this is approximately true for several hot spots which seem to be bounded at least on one side by "normal" ridge axis, i.e., hot spots whose flank slopes are not complicated by the effects of close neighboring hot spots. The Crozet hot spot, south of Madagascar, the north flank of the Tristan de Cunha hot spot and the south flank of the Azores hot spot are shown in Fig. 5 together with theoretical profiles with h_0 and x_n adjusted by eye to give the best fit. Differences between observed and theoretical profiles (Fig. 5) might reflect paucity of adequate data, inadequate averaging of observed data, barriers imposed on the flow by transform faults, or the absence of steady state conditions. Some well-surveyed hot spot profiles, such as north and south of Iceland and north of the Azores (Fig. 6A) seem more linear than concave upward, at least for small values of x. One possible explanation for this is that viscosity, μ, is not constant but increases downstream away from the hot spot; i.e. this would be expected from the downstream decrease of melt percentage and temperature, hence $\mu(x)$.

Considering that small changes in temperature and/or melt percentage could make large changes in μ, only a relatively small viscosity gradient is required to make the quadratic profiles (Fig. 5) linear, except, of course, as $x \to x_n$. To see why this is so, suppose $dh/dx = H' =$ constant < 0. Solving eq. 4 for μ, we get:

$$\mu(x) = \frac{\pi g F}{8ST\Delta\rho} \frac{H'}{(x - x_n)} \qquad (6)$$

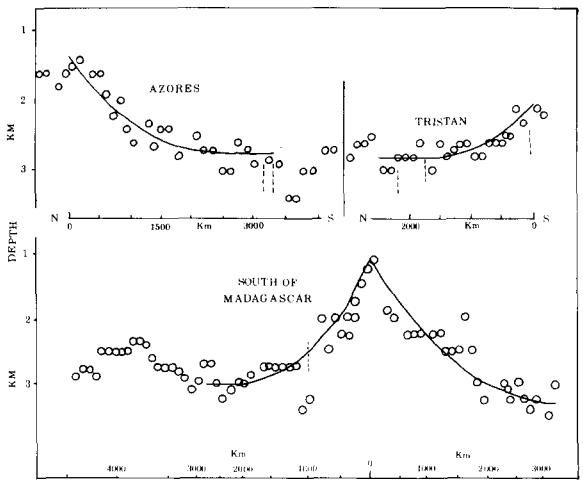

Fig. 5. Calculated (solid lines) and observed [1] axial depth profiles along Mid-Oceanic Ridge east and west from hot spot south of Madagascar, south from Azores, and north from Tristan da Cunha (Walvis–Rio Grande) hot spot. Model curves are derived by integrating a postulated requirement that pressure gradient at a point x from hot spot center is sufficient to drive enough material through the pipe to feed all the accreting lithosphere from x to x_n, the topographic limit of hot spot influence. Model curves have the form $h(x) = h_0(x/x_n)^2 - 2h_0(x/x_n) + h_0$, where h_0 and x_n were chosen to give a good visual fit to observed data. $h(x)$ is measured above apparent local undisturbed crestal elevation at some distance from hot spot. For Azores, $h_0 = 1400$ m and $x_n = 3000$ km; for Tristan, $h_0 = 750$ m and $x_n = 1500$ km; for Crozet hot spot south of Madagascar, $h_0 = 1900$ m (west) and 2180 m (east); $x_n = 2000$ km (west) and 3000 km (east).

Taking the slope of the Mid-Atlantic Ridge northward from the Azores as an example, we see from Fig. 6A that dh/dx is about the same (14×10^{-4}) at $x = 200$ km as at $x = 1000$ km. x_n is not seen north of the Azores because of interference with the southern slope away from the Iceland hot spot; however, the southern slope away from the Azores suggests x_n is at least 2000 km. From eq. 6 it follows that $\mu(x = 2000 \text{ km})/\mu(x = 200) = 1.8$. Thus, the viscosity at 1000 km need be less than twice as great as at 200 km in order for the topographic slope to be the same. If viscosity increases faster with increasing x than indicated by eq. 6, the topographic profile would be convex upward. It seems probable that viscosity is more nearly constant at great distances from the hot spot, where the Mid-Oceanic Ridge is relatively uniform along its length. If so, the topographic profile $h(x)$ predicted by the pipe model

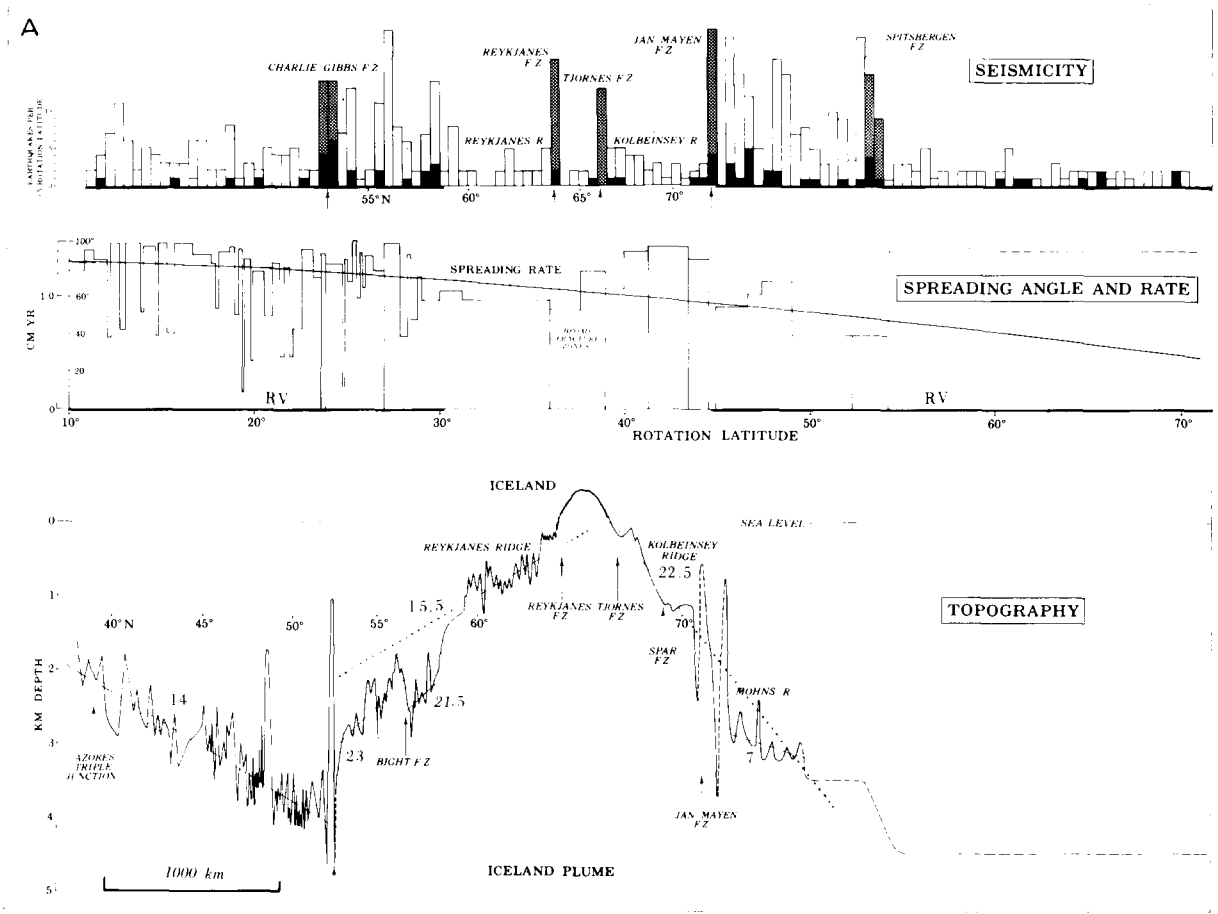

Fig. 6A. Detailed profile along the Mid-Oceanic Ridge axis through relatively well-surveyed Iceland-Azores area [5]. Seismicity, spreading angle (between local ridge axis and local normal to transform direction), spreading half-rate, and depth of immediate spreading axis are shown plotted against plate rotation latitude using late Tertiary to Recent pole averaged from the compilation of Vogt and Avery [24]. Fracture zones are indicated by arrows; earthquakes associated with fracture zones are crosshatched bars; all events of magnitude greater than 5.0 are solid; straight dashed or dotted lines and associated values ($\times 10^{-4}$) are visually fitted slopes. Part of the topographic drop south of 60°N and north of 70°N is caused by appearance of rift valley (RV; heavy line along horizontal axes). Lower seismicity is obviously associated with absence of prominent rift valley near Iceland, but the abrupt drops in seismicity north of the Spitsbergen and south of the Charlie Gibbs Fracture Zones does not seem to relate to any change in crestal morphology.

would be nearly quadratic (concave upward) far from the hot spot, linear at some middle range, and then perhaps convex upward close to the center of upwelling, where temperatures and melt percentages are high and

to comparatively great accuracy. If K and a are constant, $S/F(S)$ is a decreasing function of S, approaching a constant value as S becomes large (Fig. 4). Ther
fore the topographic slope in the direction of decreas

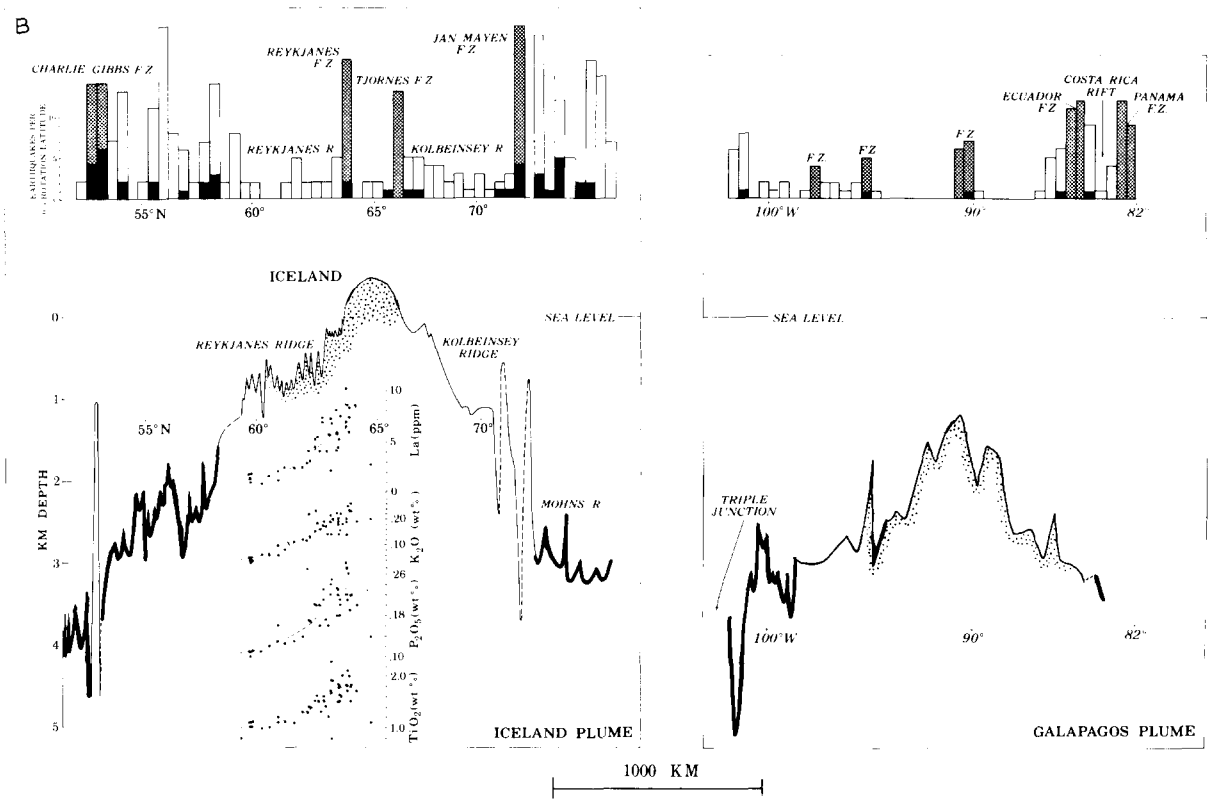

Fig. 6B. Comparison of longitudinal profiles along Mid-Oceanic Ridge through Iceland and Galapagos hot spots. Some profiles in basalt chemistry suggest the extent of the geochemical anomaly [6–8,25,28]. Chemically anomalous crust is shown stippled; its limits in the Galapagos area are derived from recent unpublished magnetic surveys, assuming that magnetic anomaly amplitudes are high in crust of high Fe and Ti concentration [27]. Topographic profile is shown by heavy line where an axial rift valley exists.

It may be that the Fe/Ti enriched zone along the Galapagos Ridge is due to fractionation [6,28], whereas such enrichment in the Iceland area might be due in part to distinct mantle plume source chemistry [7,8,10]. However, light rare earth enrichment near the Galapagos has been ascribed to plume source chemistry [13] while some authors have proposed single-source models for Iceland [26,29].

0.8 to 1 cm/yr decreases S/F by 15% (Fig. 4). Changing S from 1 to 1.2 cm/yr decreases S/F by 12%. Effects of this magnitude on the topographic slope are barely – if at all – beyond measurement uncertainty, even in the Azores and Iceland areas which are best charted. However, profiles through both of these hot spots [1] indeed seem to be steeper in a northward direction – the direction of decreasing spreading rate. We estimate these slopes from that paper and our profiles as follows: north of Iceland, 23×10^{-4}; south of Iceland (60–50°), 15×10^{-4}; north of the Azores (37–50°N), 10×10^{-4}; south of the Azores (28–38°N), 8×10^{-4}. S/F may thus at least partly explain the observed asymmetry; at least it is the only explicitly asymmetric factor in the hot spot's theoretical longitudinal profile.

Besides S, the "constants" a and K could also vary with x, and thereby alter the predicted quadratic form of the profile. Recall that:

$$F(S) = \frac{a^3K^3S^3}{a^2 + K^2S^2}, \text{ and } \frac{dh}{dx} \propto S/F$$

It is reasonable that a and K may be larger near a hot spot, since the region of partial melting is likely to be wider and deeper. The effect of increasing a and/or K is to decrease the slope. This would occur near a hot spot. Qualitatively this effect could thus also "straighten" the quadratic profile or even make it convex upward. To quantify this somewhat, let us ask what con-

ditions are imposed on a or K such that

$$\frac{dh}{dx} = H' = \text{constant } (<0)$$

Assume S is constant. From eq. 4 we then derive the condition for a linear profile:

$$\frac{8ST\mu}{S^3\pi g H' \Delta\rho}(x - x_n) = \frac{a^3K^3}{a^2 + K^2S^2} \equiv f$$

where now $a = a(x)$ and/or $K = K(x)$. As in the discussion of viscosity, we note that the equation cannot apply as $x \to x_n$; but only in some intermediate region. Taking again our earlier example of the Azores (Figs. 5 and 6A), where dh/dx at x_1 = 200 km = dh/dx at x_2 = 1000 km = H', the requirement reduces to:

$$\frac{f(200 \text{ km})}{f(1000 \text{ km})} = \frac{(x_1 - x_n)}{(x_2 - x_n)}$$

km), where the observed values are in parentheses. The calculated heights are about an order of magnitude greater than observed. (Naturally, the calculated slopes $(8T\mu S/\pi gF)\,(x - x_n)$ then also exceed the observed ones, which are in the range $10–50 \times 10^{-4}$ (Fig. 6A and other data): for x_n = 2500 km, x in the range 500–1000 km, and S in the range 1–3 cm/yr, calculated slopes dh/dx range from 6.8 to 11×10^{-3}.) Inasmuch as plate thickness, T, cannot reasonably be reduced by a factor of five, we are left with four possible alternatives:

(1) Viscosity, μ, in the pipe is about 10^{18} instead of 10^{19} P. This is certainly still within the range of possibility. Viscosity is neither accurately measurable nor likely to be constant in the pipe, and the flow might well be non-Newtonian, so the value we use is an equivalent or effective viscosity.

(2) Only the central part of the "bump" on the Mid-Oceanic Ridge is fed from the plume, the outer parts being caused by a broader region of upwelling sur-

down to $T = 40$ km is fed by passive upwelling from below, rather than nourished entirely by flow from the plume center down the conduit. If this is the case, the calculated value of h_0 will exceed the measured one (as observed) because the hydrostatic head at the plume center then does not need to be great enough to drive 100% plume-derived slush all the way to x_n, for some of the slush required for making the lithosphere would be contributed along the way. Certainly, on geochemical grounds much of the crust in the Iceland [7,8,26] and Azores [12] areas out to x_n = 1500–3000 km appears to be compositionally "depleted". The geochemical anomaly ("LIL" or large ionic lithophile element enrichment) associated with the Galapagos hot spot [6,13,27,28] does not cover the topographic bulge (Fig. 6B). Although this might mean that the "depleted" crust is produced by passive upwelling of "normal", depleted asthenosphere, it might equally imply that the plume is disgorging both kinds of ultrabasic slush, the anomalous (undepleted) kind upwelling only in the core of the convection cell [5]. If the LIL-enriched core is narrow (say 50 km diameter), it is perfectly possible that both kinds of material are injected into the pipe, the LIL-enriched above the depleted. Another possibility is that *both* depleted and anomalous partial melts are formed by the same fractionation process (near the plume center) [26,29]. In support of this we observe that *exceptionally* LIL-depleted basalts occur on the distal flanks of several hot spots, including Iceland and the Galapagos ([6,28], and work in preparation). These basalts apparently come from partial melts stripped of LIL elements near the plume center. Both of these possibilities would explain why the geochemical anomaly covers only a central fraction of the hot spot's topographic bulge (Fig. 6B). The latter possibility is difficult to reconcile with the $^{87}Sr/^{86}Sr$ data, however [10].

In summary, we have proposed that the topographic profile along the axis of the Mid-Oceanic Ridge, crossing over a hot spot, may reflect the requirement that the horizontal pressure gradient at a point x is adequate to deliver the material needed to make all the new near-axial lithosphere out to x_n, the limit of the flow. Any increase in discharge would make a proportional increase in x_n, at the same time increasing dh/dx at any x, and h_0. Starting from this requirement, we showed that the topographic profiles $h(x)$ should be quadratic and concave upward, at least for hot spots without close neighbors. Some observed profiles do seem to fit this model (Fig. 5), whereas others are more linear or even slightly convex upward (Fig. 6A, B). This departure from the model could easily be explained as resulting from modest downstream increases in viscosity or decreases in the cross-dimensions of the pipe. We then examined whether the hot spot heights, h_0, are consistent with the model for reasonable choices of constants. The calculated h_0's were about a factor of five too high if $T = 40$ km, $\mu = 10^{19}$ P, $K = 1.24 \times 10^{14}$ sec (estimated from Solomon [19]), $a = 20$ km, and observed x_n are used. Rather than abandoning the simple but illuminating analytical model, we proposed that this discrepancy could easily be explained if one of the following are true: (1) viscosity is closer to 10^{18} P; (2) $K = 3.7 \times 10^{14}$ sec (a compromise between the values implied by Leeds et al. [20] and Solomon [19]); (3) lithosphere is "plume-derived" only out to 500 or 1000 km, i.e. Schilling's geochemical anomaly [7,12], rather than the entire observed topographic bulge; or (4) some of the lithosphere out to x_n is fed by passive upflow from below, rather than derived from the plume, or (5) some combination of the above factors.

4. Hot spot heights versus spreading rates: implications of the plate feed hypothesis

In the previous discussion we showed how longitudinal profiles of ridge-centered hot spots could be derived by integrating the condition that slope at any point be sufficient to "feed" the growing plate downstream from that point (the "plate feed hypothesis"). We show now that this also leads to a predicted $h_0(S)$ which is not quite the same as the expression we derived in the first section of this paper. Recall that in the first section we did not assume the pipe flow fed the plate except in the immediate hot spot area. We also took $x_n \simeq$ constant or randomly variable, which would be consistent with the small number of examples.

Assume first that there is no correlation between plume discharge Q and spreading rate. This is the "passive flow" hypothesis for flow below the ridge (Alternatively, if plumes help drive plates, there may be a tendency for plume discharge to be higher on fast ridges, all else being equal.) Suppose also that all, or a

down the pipe and is used up to make new plate. If all discharge ends up making new plate, then the influence of plumes on slow ridges must extend further down the pipe than that of plumes on fast ridges, because then discharge, $Q = 4TSx_n$, which could be taken to be either constant, randomly variable, or tending to increase with increasing S. Solving for x_n, introducing this into the expression for h_0 (derived from eq. 5 by

10^{14} sec (instead of 1.24×10^{14} sec) and the curve is similarly constrained to pass through $h_0 = 2.6$ km at $S = 1$ cm/yr, $F(S)$ is changed from F_1 to F_2 (Fig. 4) and the appropriate value of Q_0 is 2.5 km^3/yr. The resulting curve is not significantly different (Fig. 2); the viscosity required for this combination of parameters is 0.5×10^{19} P, close to the value implied by the speed of asthenosphere motion deduced from V-shaped

referred to such highs as hot spots or plumes, although the depth of origin and other properties of the upwelling material is still conjectural. The evidence for gradual plate thickening with increasing crustal age is now rather strong [15,16,20]; on the basis of this evidence we postulate that the pipe-like region of extensive partial melting that must exist below the plates in the vicinity of the spreading axis [3,7,19,21,32] is essentially constant in vertical thickness but in its width is proportional to spreading rate. An additional effect, cess to "bleed" down the pipe under low topographic – hence pressure – gradients. We propose that this is why there are no Iceland- or Azores-like topographic highs on fast-spreading ridges. The predicted dependence of hot spot heights on spreading rate gives a rather good fit to the data (Fig. 2), all things considered. Note that if there were localized downwellings on the Mid-Oceanic Ridge – the "discordance" south of Australia may be such a place [34] – the same reasoning would apply, namely the deepest "saddles"

feeds the accretion process; this model was first suggested by Schilling [7]; (b) chemically anomalous material forms only the core of the plume and ends up in the higher parts of the horizontal pipe. Normal mantle entrained along the margin of the plume ends up deeper in the horizontal pipe and "surfaces" further downstream. This model also includes the possibility that both normal and depleted materials form by partial melting and fractionation processes from the same parent magma in the area of upwelling [26,29].

In our discussion we assumed a steady-state hot spot where the topographic profile has adjusted itself to provide sufficient gradient to carry the plume influx away. In other words, our model is that of a mountain with a well at the top and pipes running down the flanks. (The partial melts flow downhill under the action of gravity; they are not "forcefully injected" as suggested by Schilling [7,8,11].) But how does this "mountain" in the asthenosphere below the plates, and perhaps also in the mesosphere, come into being? We visualize the process as follows: suppose a plume is "turned on" at some time, before which the mid-oceanic pipe is horizontal. The excess plume discharge will flow into the existing pipe, probably the upper part since plume materials are of lower density. This makes the existing pipe thicker. But since the lower edge of the pipe (actually a broad transition zone!) is pressure-controlled [7,32], it will reconsolidate as melt concentrations are reduced by the increasing overburden pressure. In this fashion partial melts previously in the pipe-like region of low viscosity will be converted back to normal asthenosphere of low melt percentage and somewhat greater viscosity. At greater depths normal asthenosphere is reconverted to mesosphere. Thus the process of pipe flow could build its own mountain; the initially steep gradients will smooth out as partial melts spill further downstream; finally a quadratic-like equilibrium profile is reached (Fig. 5).

The pipe flow model neglects "radial" outflow from the hot spot into the normal asthenosphere. Such flow probably exists, but flow speeds in the "normal" asthenosphere will be reduced (perhaps speeds there are of the order a few cm/yr) by the lower melt percentage (perhaps a few percent) [30,32] and consequent higher viscosity. A component of radial flow would help "cause" plate tectonics [14], both by viscous drag and by creating a nonisostatic bulge from which the plates can slide. In part, such radial flow helps explain why the gravity and depth anomalies extend over large areas away from the spreading axis. Part of the persistently elevated sea-floor produced by elevated ridges near hot spots [35,36] may reflect higher initial plate temperature, higher asthenosphere temperature, and, as a reflection of this, a plate more effectively fractionated and therefore enriched in low-density phases.

A significant correlation between free-air gravity anomaly and elevation anomaly along the Mid-Oceanic Ridge [1] supports our hypothesis that mantle material is upwelling below the elevated areas; the plates are not strong enough to support the loads implied by the mass excess responsible for the gravity anomaly [1]. However, the results of this paper must qualify the conclusion of Anderson et al. [1] who "found no correlation between spreading rate and gravity and no uniform relationship which holds in all the oceans between spreading rate and observed crestal depths". We find that minimum regional depth on the Mid-Oceanic Ridge depends inversely (and nonlinearly) on spreading rate. Maximum regional depth, on the other hand, is essentially independent of spreading rate; it is the normal crestal depth, usually about −2.9 km, which obtains far from hot spot influence. This conclusion is evident in our Fig. 2; the insert in this figure represents all 500 km averages of crestal depth and was taken from Fig. 4 of Anderson et al. [1], who also noticed that "all the variability of the crestal elevation occurs on slow-spreading ridge". Our pipe flow model explains this observation.

If crestal elevation relates to spreading rate while gravity relates to crestal elevation, then gravity should relate to spreading rate. Yet, Anderson et al. [1] found no overall significant correlation between the latter two quantities. We explain this apparent contradiction as follows: Inspection of the world gravity pattern [37] (Fig. 1) together with topographic and geologic charts shows clearly that there are many gravity features unrelated to any obvious crustal patterns, whereas other anomalies do relate. The total gravity pattern must therefore be a superposition of "signal" and "noise" components. The "signal" consists of anomalies related to crustal features, such as the highs over various major hot spots, even though the source for such crustal features in general must be in the mantle. The "noise" consists of density anomalies of unknown

origin, possibly related in some way to convection in the asthenosphere and deeper mantle. On fast-spreading ridges no high mass excesses accumulate in hot spot areas, and the gravity "signal" remains low, while – apparently – the "noise" remains. On slow ridges like

off the plume discharge rising from below. Such extreme mass excesses would be accompanied by equally extreme gravity potentials available to the two plates involved; this would make the two plates slide apart faster, thereby widening the conduit, bleeding off more

to stand out; in fact, Anderson et al. [1] find a positive correlation (at 95% confidence) between gravity and spreading rate in those oceans. If there were some way to remove the "noise" component from the gravity map, and at the same time consider only the hot spot

related process is radial flow of plume discharge into the asthenosphere [2]. As spreading rates decline and the mid-oceanic artery begins to clog, the potential available to force partial melts at right angles to the ridge crest increases. The traction exerted by such flow

plume centers at such high rates. Despite the above speculations about causality, we stress once more that considerations of causality are not part of the assumptions for this paper, but merely a promising ramification.

Acknowledgments

I thank J.G. Schilling, W.J. Morgan, H.C. Eppert, Jr., A. Ballard and G.L. Johnson for review; and S. Edwards, B. Wells, F. Hubbard and N. Hunt (all from the U.S. Naval Oceanographic Office) for assistance. This work was partly supported by the Office of Naval Research.

References

1 R.N. Anderson, D. McKenzie, and J.G. Sclater, Gravity, bathymetry, and convection in the Earth, Earth Planet. Sci. Lett. 18 (1973) 391.
2 P.R. Vogt, Asthenosphere motion recorded by the ocean floor south of Iceland, Earth Planet Sci. Lett. 13 (1971) 153.
3 P.R. Vogt and G.L. Johnson, Transform faults and longitudinal flow below the Mid-Oceanic Ridge, J. Geophys. Res. 80 (1975) 1399.
4 P.R. Vogt and G.L. Johnson, Mantle plumes and transform fractures, Trans. Am. Geophys. Union 54 (1973) 239.
5 P.R. Vogt, The Iceland phenomenon: imprints of a hot spot on the ocean crust, and implications for flow below the plates, in: Geodynamics of Iceland and the North Atlantic Area, ed. L. Kristjansson (NATO Advanced Study Institute, Reykjavik, 1974) in press.
6 P.R. Vogt, R.N. Hey, G. Byerly, J. DeBoer, and A. Trehu, Magnetic telechemistry, sub-axial flow, and the Galapagos hot spot: new observations, Trans. Am. Geophys. Union 56 (1975) 445.
7 J.G. Schilling, Iceland mantle plume: geochemical study of Reykjanes Ridge, Nature 242 (1973) 565.
8 J.G. Schilling, Iceland mantle plume, Nature, 246 (1973) 141.
9 J.G. Schilling, Afar mantle plume: rare-earth evidence, Nature Phys. Sci. 242 (1973) 2.
10 S.R. Hart, J.G. Schilling and J.L. Powell, Basalts from Iceland and along the Reykjanes Ridge: Sr isotope geochemistry, Nature Phys. Sci. 246 (1973) 104.
11 J.G. Schilling and A. Noe-Nygaard, Faeroe-Iceland plume: rare-earth evidence, Earth Planet. Sci. Lett. 24 (1974) 1.
12 J.G. Schilling, Azores mantle blob: rare-Earth evidence, Earth Planet. Sci. Lett. 25 (1975) 103.
13 J.G. Schilling, R.N. Anderson and P.R. Vogt, Rare-earth variations along the Galapagos spreading center, 101°–83°W: a pilot study, Trans. Am. Geophys. Union 56 (1975) 469.
14 W.J. Morgan, Deep mantle convection plumes and plate motions, Bull. Am. Assoc. Pet. Geol. 56 (1972) 203.
15 P.R. Vogt, Evidence for global synchronism in mantle plume convection, and possible significance for geology, Nature 240 (1972) 338.
16 P.R. Vogt, Volcano height and plate thickness, Earth Planet Sci. Lett. 23 (1974) 337.
17 P.R. Vogt, E.D. Schneider and G.L. Johnson, The crust and upper mantle beneath the sea, in: The Earth's Crust and Upper Mantle, ed. P.J. Hart, Am. Geophys. Union Monograph 13 (1969) 556.
18 K.F. Scheidegger, Temperatures and compositions of magmas ascending along mid-ocean ridges, J. Geophys. Res. 78 (1973) 3340.
19 S.C. Solomon, Shear wave attenuation and melting beneath the Mid-Atlantic Ridge, J. Geophys. Res. 78 (1973) 6044.
20 A.R. Leeds, L. Knopoff and E.G. Kausel, Variations in upper mantle structure under the Pacific Ocean, Science 186 (1974) 141.
21 S.C. Solomon and B.R. Julian, Seismic constraints on ocean-ridge mantle structure: anomalous fault-plane solutions from first motions, Geophys. J.R. Astron. Soc. 38 (1974) 265.
22 H. Lamb, Hydrodynamics (Dover, New York N.Y. 1945) 738.
23 P.R. Vogt and G.L. Johnson, A longitudinal seismic reflection profile of the Reykjanes Ridge, II. Implications for the mantle hot spot hypothesis, Earth Planet. Sci. Lett. 18 (1973) 49.
24 P.R. Vogt and O.E. Avery, Tectonic history of the Arctic basins: partial solutions and unsolved mysteries, in: Marine Geology and Oceanography of the Arctic Seas, ed. Yvonne Herman (Springer Verlag, New York, N.Y., 1973) in press.
25 J. Campsie, J.C. Bailey, M. Rasmussen and F. Dittmer, Chemistry of tholeiites from the Reykjanes Ridge and Charlie Gibbs Fracture Zone, Nature Phys. Sci. 244 (1973) 71.
26 G.E. Sigvaldason, S. Steinthorsson, N. Oskarsson and P. Imsland, Compositional variation in recent Icelandic tholeiites and the Kverkfjoll hot spot, Nature 251 (1974) 579.
27 P.R. Vogt and G.L. Johnson, Magnetic telechemistry of oceanic crust?, Nature 245 (1973) 373.
28 G.R. Byerly, W.G. Melson and P.R. Vogt, Extreme differentiation of ocean ridge volcanic rocks: Galapagos Ridge and Juan de Fuca Ridge, Trans. Am. Geophys. Union 56 (1975) 469.
29 R.K. O'Nions and R.J. Pankhurst, Secular variation in the Sr-isotope composition of Icelandic volcanic rocks, Earth Planet. Sci. Lett. 21 (1973) 13.
30 N.H. Sleep, Segregation magma from a mostly crystalline mush, Geol. Soc. Am. Bull. 85 (1974) 1225.
31 A.H. Lachenbruch, A simple mechanical model for oceanic spreading centers, J. Geophys. Res. 78 (1973) 3395.
32 R. Kay, N. Hubbard and P. Gast, Chemical characteristics

and the origin of oceanic ridge volcanic rocks, J. Geophys. Res. 75 (1970) 1585.
33 R.L. Post, Jr. and D.T. Griggs, The earth's mantle: evidence of non-Newtonian flow, Science 181 (1973) 1242.
34 J.K. Weissel and D.E. Hayes, The Australian-Antarctic discordance: new results and implications, J. Geophys. Res. 79 (1974) 2579.
35 P.R. Vogt and O.E. Avery, Detailed magnetic surveys in the northeast Atlantic and Labrador Sea, J. Geophys. Res. 79 (1974) 363.
36 J.G. Sclater, L.A. Lawver and B. Parsons, Comparison of long-wavelength residual elevation and free air gravity anomalies in the North Atlantic and possible implications for the thickness of the lithospheric plate, J. Geophys. Res 80 (1975) 1031.
37 W.M. Kaula, Global gravity and tectonics, in: The Nature of the Solid Earth, ed. E.C. Robertson (McGraw-Hill, New York, N.Y., 1972) 385.
38 S.C. Solomon and N.H. Sleep, Some simple physical models for absolute plate motions, J. Geophys. Res. 79 (1974) 2557.
39 R.L. Parker and D.W. Oldenburg, Thermal model of ocean ridges, Nature Phys. Sci. 242 (1973) 137.